Advances in Science and Technology Research Journal

Advances in Science and Technology Research Journal 2024, 18(4), 265–272
https://doi.org/10.12913/22998624/189290
ISSN 2299-8624, License CC-BY 4.0

Received: 2024.04.30
Accepted: 2024.05.24
Published: 2024.06.20

The Role of Cathode Heat in the Schottky Correction in the Ionization Layers of Arc Plasma

Tapark Abdlraheem Saber[1], Rafid Abbas Ali[1*], Huda Muhammad Jawad[1]

[1] Department of Physics, College Science, Mustansiriyah University Baghdad, Iraq
* Corresponding author's e-mail: rafidphy_1972@uomustansiriyah.edu.iq

ABSTRACT

Enhancing lighting intensity while reducing costs is a primary focus. Lamp illumination has been refined by adjusting halide concentrations and pinpointing optimal thermal zones for maximum brightness. Arc discharge, particularly in high-intensity discharge (HID) lamps, plays a pivotal role in lighting technology and system upgrades. This study delves into the plasma processes of the ionization layers near the cathode surface, where we noticed that as the temperature increases, both (T_e, Δ_A, $\varnothing_b$) increase, also, notice an increase in the voltage barrier as a result of the collision between the electrons that leads to a loss of energy, and this leads to a decrease in the current density as a result of the high energy gap. That is, the value of the work function increases As a result of the increase in the energy of the electrons, which plays a major role in the processes of ionization and excitation, this is reflected in an increase in the temperature of the electron and a decrease in the voltage, especially at a voltage of 20 V, meaning that increasing the voltage difference from 10 to 20 V leads to a significant decrease in the voltage barrier, especially at temperatures greater than (T_w = 3800 K), and this leads to increase the temperature of the electron as a result of increasing the energy of the electrons so, at low temperatures, we notice that the effective work function increases in both cases (10.20) V with the decrease in the potential difference of the plasma layers at the cathode surface proximity, and it has a maximum value at 20 V. The difference in concentration plays a crucial part in increasing the temperature and decreasing the voltage barrier with the difference in the applied voltage

Keywords: voltage barrier, schottky correction, electron temperature.

INTRODUCTION

The phenomenon known as arc discharge is a gas discharge that happens when current flows through an air-like dielectric medium. It is a self-sustaining discharge phenomenon that is characterized by immediate spark production [1]. The insulation of the surrounding gas breaks off, creating an electric arc that causes a continuous discharge and current to flow through a non-conductive material. An electrical brief is the idea of an electric arc [2]. There are several uses for arc discharge in the lamp industry. It may be utilized to make long-arc discharge lamps that have a long lifespan and a long effective light emission length [3]. This is accomplished by utilizing a luminescent tube that has distinct UV transmittance in various regions, such as the central region's first luminous tube portion and the ends' second and third luminous tube portions [4] Long arc discharge lamps can also be made to reduce thermal stress that has accumulated inside the arc tube [5]. To do this, a hollow section of the arc tube that is in touch with both the electrode and the tube's edge is created around the electrode [6] The significance of boosting plasma discharge at low temperatures in industrial settings was examined by the researcher Lieberman Michael A and et al, with a focus on the production of semiconductors and plasma display panels for high-definition televisions [7]. Utilizing concentration with gases, the researcher Cornella Roca and et al conducted an overview of the uses of electrically produced plasma for surface treatment in materials science. The production of superior nanomaterials with a crystalline state and certain functional

characteristics, such as structures and nanoparticles, is accomplished using atmospheric arc discharge techniques [8]. The lightning strike in a plasma burner was the primary focus of the researcher Stoffels Eva et al. The plasma's and the electrodes' thermodynamic and electromagnetic interaction was studied using a model and electrode areas, and the conclusions mostly agreed with experimental data [9]. The researcher Liang Peng et al produced low-dimensional carbon nanoparticles, such as graphite nanosheets, using pulsed arc discharge [10]. To address surfaces in materials science, the researcher Coebella Carles et al employed a review of the uses of electrically produced plasma employing concentration with gases [11]. The investigator Li, Tiah Ming, et al employed a light. tungsten electrodes in a long-arc discharge system that stops the emitting material from spreading and the inner wall of the lit tube from becoming black [12]. A long-lasting short arc discharge light was utilized by the researcher Scholand, Michael et al. The lamp is made out of a bright tube with an interior closed section that creates a discharge gap. At the top and lower extremities of the discharge space, the anode and cathode are positioned in opposition to one another. The lamp's purpose is to keep the illumination surface from getting too dark and to extend its lifespan [13]. This research aims to study the effect of the cathode temperature on the voltage barrier and the electron temperature. The Schottky correction was also studied for different concentrations and to determine the appropriate conditions for manufacturing the best light bulb at a lower cost and a simple temperature.

THEORETICAL PART

If function $U(w, d)$ is known, the distribution of temperatures inside and outside the cathode structure may be determined by figuring out the heat conduction formula [14]:

$$\nabla(K\nabla T) = 0 \tag{1}$$

where: K a shift in temperature ∇T. The cathode material's thermal conductivity.

There is a boundary situation.

$$k\frac{\partial T}{\partial n} = q\,(T_w, U) \tag{2}$$

where: q – energy flux density, T_w– cathode surface temperature, U – the low combined voltage amid the ionization layer and the charge sheath.

When the limits condition, cold gas, and arc plasma come into touch with the surface of the cathode. in this case, n is a local orientation perpendicular to the cathode's surface that points away from it [15]:

$$T = T_c \tag{3}$$

where: T_c– temperature of the cathode, within the context of this model, the energy flow density, *qp*, generated by plasma at the surface of the cathode is expressed by the formula that follows [16]. The formula defines α as the proportion of the mean free path for ion-atom collisions to the ionization length [17]:

$$\alpha = \sqrt{\frac{2}{3}}\frac{C_{ia}Q_{ia}}{K_i} \text{ and } C_{ia} = \sqrt{\frac{8KT_h}{\pi}}\left(\frac{1}{m_i}+\frac{1}{m_a}\right) \tag{4}$$

where: k_i and Q_{ia}– symbolize the rate of change of atom the gas's ionization under consideration as well as the average cross-section for elastic ion-atom collision momentum transfer, C_{ia} – refers to the average relative atom and ion speed within the instance within the plasma created in the single-atom pure gas [18]. Within the context of this paradigm, the energy flux density q_p generated by plasma at the cathode's exterior is expressed using the subsequent formula [19].

$$q_p = q_i + q_e - q_{em} \tag{5}$$

where: q_i – the density energy flow around the cathode interface via ions, q_e – the energy flow cathode Surface density by swift electrons in the plasma. q_{em} – density of energy flux lost from the surface of the cathode by thermal emission.

$$qi = j_i\,[\,Z_eU_D + E - ZA_{eff} + + k(2T_h + -2TW) \tag{6}$$

where: j_i that the electric current density of the ions provides the cathode surface, T_h – heavy particle temperature (ions, neutral particles), T_e – temperature of the electrons in the stratum close to the cathode. Z – the rate of the number of charging ions, E – the average of the layer's ionization energy near the cathode, U_D – low voltage within space charge envelop, A_{eff}– work function (Schottky correction).

$$q_e = J_e\left(2KT_e + A_{eff}\right) \quad (7)$$

$$q_{em} = J_{em}\left(2kT_w + A_{eff}\right) \quad (8)$$

where: j_e – how dense the electric current is transmitted by the use of the cathode surface fast plasma electrons, J_{em} – electron emission density at the moment, $j_e = eJ_e$ is the quantity of ions that provide a voltage to the cathode's electrical surface, $J_{em} = eJ_{em}$ is the thermionic emission current density. $ji = Z_e j_i$ is the quantity of ions that provide an electrical flow across the cathode's surface, which was computed with the Schottky correction taken into account.

Indicate the electric field's W_i work above the ions in the layer of ionization. W_i is approximated as the average current of ions in the model framework, the layer of ionization $j_i/2$, periods $U_i = U - U_D$ the ionization layer voltage decrease (given by Equation) Equation 6 might be rephrased as [20].

$$q_i = J_i\left(Z_e U_D + E - ZA_{eff}\right) + W_i + \\ + \left[j_i k\left(2\,T_h + \frac{ZT_e}{2}\right) - (j_i 2kT_w) + W_i\right] \quad (9)$$

where: T_h – heavy particle temperature (ions, neutral particles), T_e – temperature of the electrons in the stratum close to the cathode, Z – the rate of the number of charging ions, E – the average energy of ionization inside the layer near the cathode, U_D – reduced voltage within the space charge envelope, A_{eef} work function (Schottky correction), W_i – low voltage in the ionization layer, U_D – low voltage in the space charge envelope.

Equation 9 represents the flow of ions' energy into the sheath from the ionization layer. The total energy flow of the electric field's work over the ions in the ionization layer is the second term. and of the atoms with the same energy that is neutral and enter the ionization layer that follows, they depart the cathode surface. being generated to counteract the incoming ions. All of these parameters need to be equal in a steady. In actuality, the equation balancing the ionization layer's heavy particle energy is represented via the state need for these terms to be equivalent.) As a result, formula 9 should have its final word located on the right removed, and it now has the form [12]:

$$q_i = J_i\left(Z_e\, U_D + E - Z\, A_{eff}\right) + W_i \quad (10)$$

In actuality, the Equation the ionization layer's heavy particle energy balance is represented by the state need for these terms to be equivalent.) As a result Equation 9 should have its final word located on the right removed, and it now has the form [22]:

$$Je\left(2\frac{KT_e}{e} + U_D\right) + 3.2j\frac{KT_e}{e} + j_i E \quad (11)$$

$$jem\left(2\frac{KT_e}{e} + U_D\right) + w_e \quad (12)$$

Here, is the ionization layer's electrons under the influence of the electric field, and is the net electric current density that flows from the plasma to the surface. Keep in mind that the words located on the left refer to that flow of energy transported by swiftly moving electrons from the ionization layer into the sheath, which are sinks of the electron in the ionization layer's energy. that flow the electron energy lost within the ionization layer and the energy moved about away with electrons departing the layer for the main plasma. The terms located on the right represent sources, the electric field's activity across the electrons inside the stratum, and the energy delivered into the layer made of expelled acceleration of electrons within the space-charge sheath. Equation 5 may be produced by substituting Equations 8 and 10, adding the acquired connection to Equation 11, and using the formula.

$$q_p = J_U - \frac{j}{e}\left(A_{eff} + 3.2K\,T_e\right) \quad (13)$$

where: e – change of electron, j – current density, U – the low combined voltage amid the layer of ionization and the charge sheath.

There is a clear physical meaning to the Equation 13. The energy flux related to the plasma that reaches It is the cathode surface the difference between the electrical power deposited in the near cathode layer per unit area and the force carried by a current carrying electrons from the layer into the bulk plasma, the latter is computed with consideration for the energy required to extract the cathode's electrons. Evidently, applying Equation 13 results from substituting Equation 10 for Equation 7. Equation 17 – the potential energy of the electron barrier that occurs at the junction of a semiconductor refers to the metal as the Schottky barrier [22]. When a metal comes into direct contact with a semiconductor, a Schottky barrier forms, resulting in proper electrical contact behavior provides the height of the

barrier, which is easily computed from the difference between the metal's work function and the semiconductor's electron affinity [23]:

$$\phi B_n = \phi_m - x \tag{14}$$

where: ΦB_n – the energy barrier of the electrons. The difference, as expressed in the equation, between the electrons' energy barrier and the semiconductors' energy gap [24].

$$\phi Bn = Egap - \phi Bn \tag{15}$$

The energy gap of semiconductors is represented by, and the electron energy barrier by ϕBn. The following formula is used to calculate the delivery value [25]:

$$J_{th} = A^{**}T^2 e - \frac{\phi B_{n,p}}{k_b T}\left(\frac{qv}{e^{kbT}} - 1\right) \tag{16}$$

The Equation provides the height of the voltage barrier [25]:

$$\phi_B = kT/qln\left[\frac{A^*T^2}{J_S}\right] \tag{17}$$

where: Φ_B– the voltage barrier kT/q – is the volt equivalent of temperature, J_s – is the saturation current density.

RESULTS

This study examines the correlation between cathode temperature (T_w) and potential barrier length ($Øb$), as depicted in Figure 1. At a voltage of U = 10 V, electron emission initiates within the temperature range of 20–5000. As concentrations (0.001, 0.01, 0.1, 0.5) rise, there is a proportional increase in emitted electrons, indicating that higher temperatures significantly impact the density of liberated electrons resulting from electron molecule collisions. This, in turn, reduces the voltage barrier. In the case of shape (b), higher voltages (U = 20 V) produce stronger electricity, characterized by a shorter potential barrier and increased electronic emission due to a higher electric field. Consequently, at elevated temperatures (4000–6000), more ionization processes occur, further reducing the potential barrier. Moreover, with increasing concentrations (0.1, 0.5), the potential barrier diminishes due to heightened ionization processes, leading to increased collisions and, consequently, higher electron emissions. The data presented in Figure 2 illustrates that electron emission initiates at 500° under a voltage of U = 10 V. As the temperature escalates from 3800–5000, induced by the ionization process, there is a noticeable augmentation in electron temperature, leading to intensified collisions between electrons and molecules. Amplifying the voltage to (U = 20 V) further enhances the electric field, resulting in a temperature range of 3300–5000 and heightened electron emission, consequently elevating (Te). Introduction of concentrations (0.001, 0.01, 0.1, 0.5) prompts a marked rise in electron temperature at concentrations (0.1, 0.5), as electrons acquire energy from collisions with other particles, including atoms and neutral ions. The likelihood of collisions rises with the concentration of these molecules. Increased electron temperatures are attributable to energy transfer during collisions, augmenting the kinetic energy of the electrons. Figure 3 depicts the Schottky barrier's value for pure material, measured at 1.2 eV, when the temperature (T_w) is 3000 K. This value is notably smaller than U_i, which stands

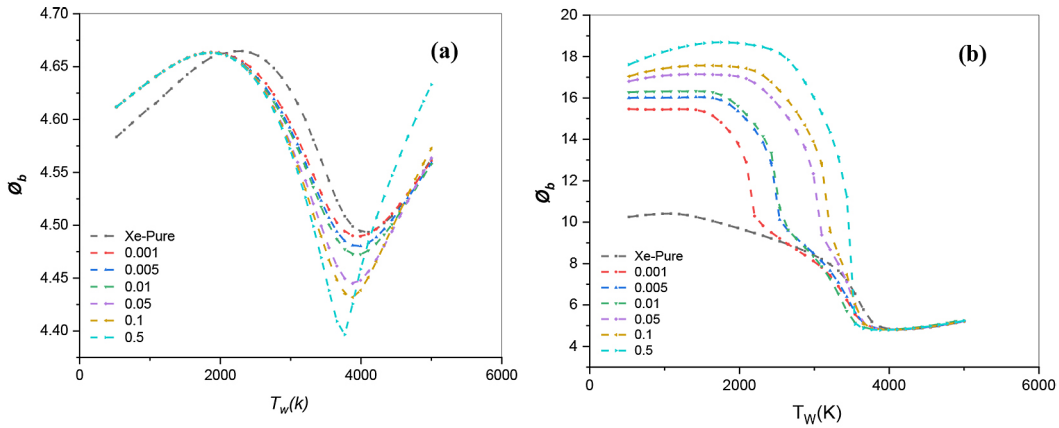

Figure 1. Voltage barrier versus the cathode temperature for all concentrations (a) U = 10 V, (b) U = 20 V

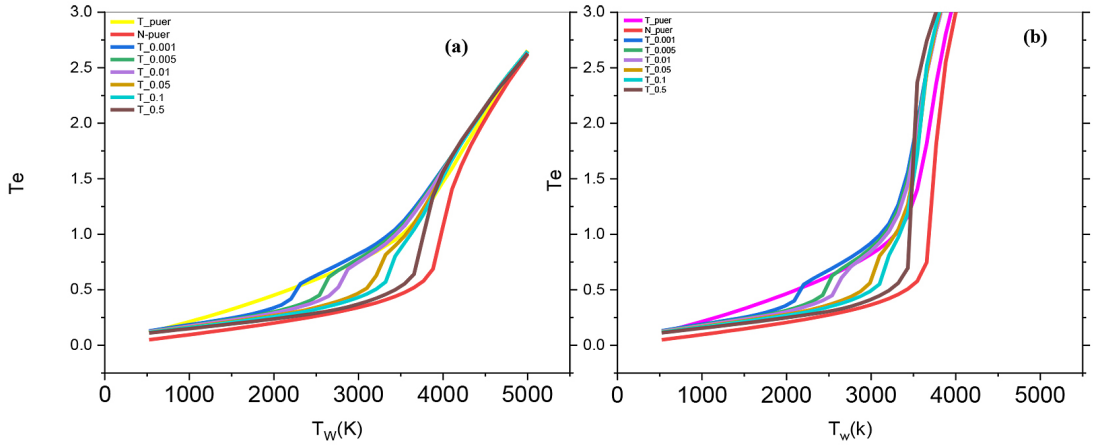

Figure 2. Voltage barrier versus the cathode temperature for all concentrations (a) $U = 10$ V, (b) $U = 20$ V

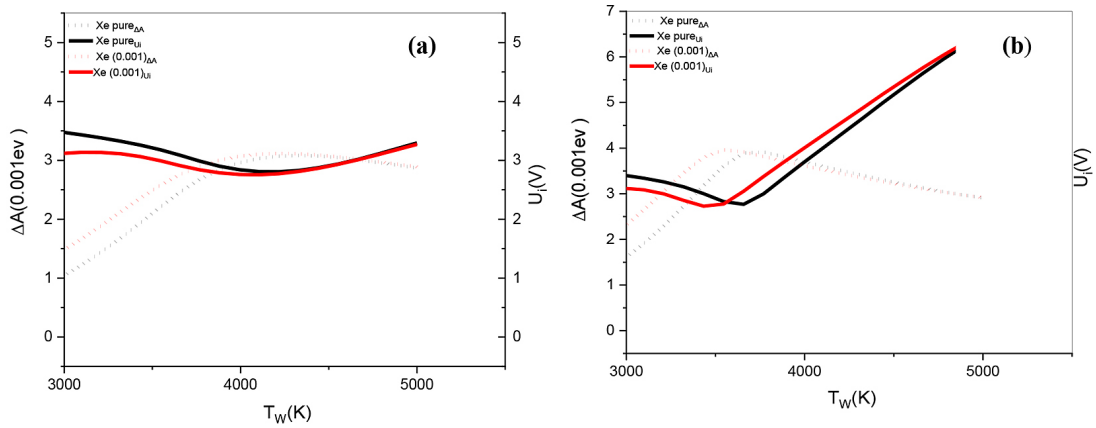

Figure 3. Schottky correction and ionization voltage versus cathode temperature for concentration (0.001) (a) $U = 10$ V, (b) $U = 20$ V

at 3.4 V, indicating insufficient thermal energy to facilitate electron passage across the barrier. Conversely, with a concentration addition of 0.001 at T_w = 4000 *K*, the energy gap contracts, augmenting the Schottky Correction due to increased electron concentration. This facilitates electron movement across the barrier and onto the metal surface, leading to an increased Schottky correction of 1.5 eV attributed to ion release activities at higher temperatures. Consequently, the potential difference between potential layers near the cathode (*Ui*) decreases. As voltage increases, exemplified at $U = 20$ V and T_w = 4100 K, the barrier rises to 1.6 eV, consistent with the heightened ionization layers at *Ui* = 3.3 V. Furthermore, the addition of concentration leads to a rise in Schottky correction, resulting in a definite decrease in U_i at T_w = 3500 K.

Figure 4 shows that, in pure xenon, the Schottky value (effective work function) is small at 1.2 eV at a certain heat of T_w = 3000 K. At the same temperature, the potential difference of the ionization layers (3.5 volts) increases clearly with the small value of the function. Work when adding the concentration (0.01), we see that at the voltage U = 10 V, the Schottky correction will rise as a result of collisions and the release of electrons, which will raise the value of the current. The Schottky value appears at (2.5 eV). The voltage will be 2.4 V at a temperature of 4100 K. As with the Schottky drop before concentration, the ionization potential will rise at $U = 20$ V, and the opposite will occur when concentrations are added. see an increase in Schottky correction at $U = 20$ V compared to the previous voltage $U =$ 10V. In Figure 5, a significant difference in the Schottky Correction value is evident between previous concentrations, where it was 1.1 eV, a notably low figure corresponding to a substantial increase in the ionization potential to 3.5 eV at

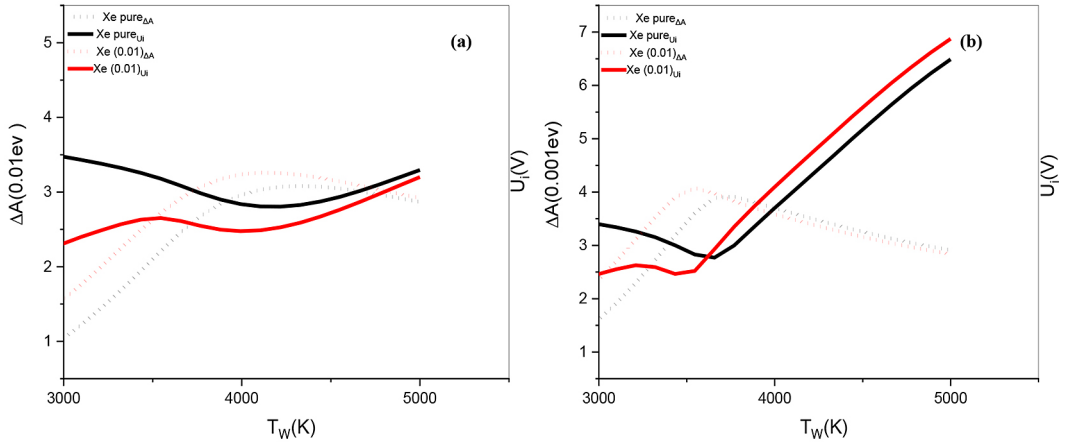

Figure 4. Schottky correction and ionization voltage versus cathode temperature for concentration (0.01), (a) $U = 10$ V, (b) $U = 20$ V

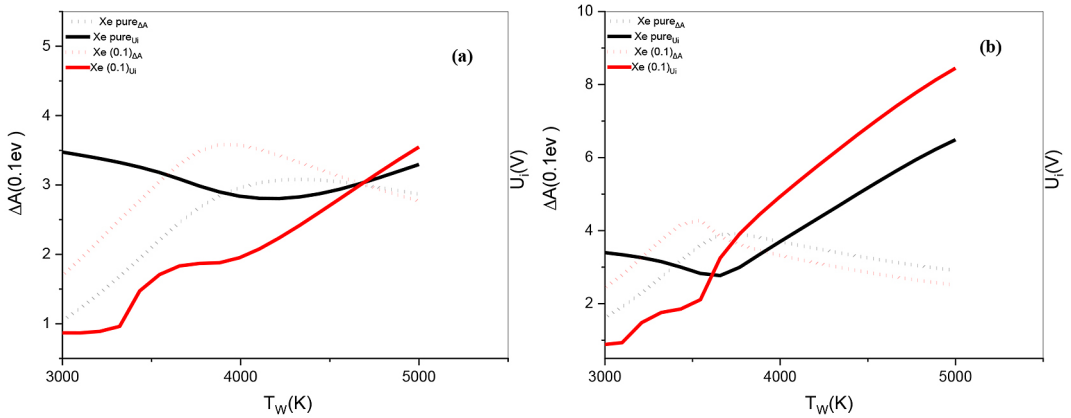

Figure 5. Schottky correction and ionization voltage versus cathode temperature for concentration (0.1), (a) $U = 10$ V, (b) $U = 20$ V

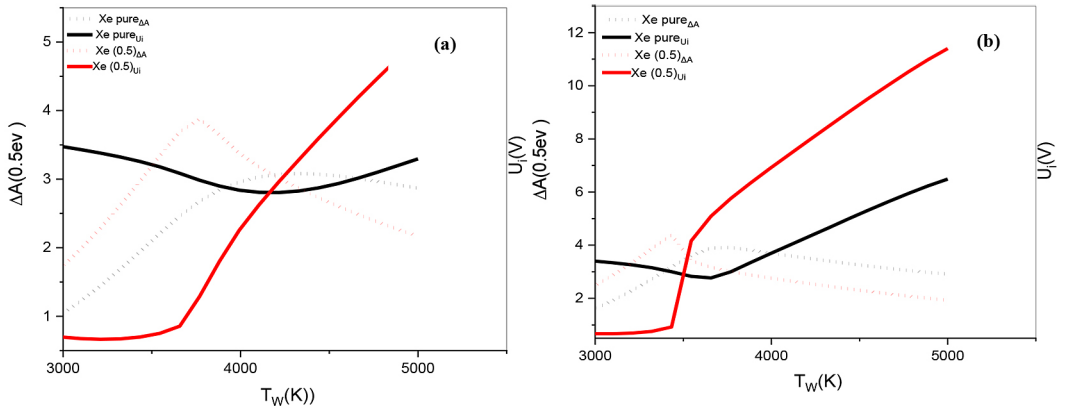

Figure 6. Schottky correction and ionization voltage versus cathode temperature for concentration (0.5), (a) $U = 10$ V, (b) $U = 20$ V

a temperature of $T_w = 3000$ K. Conversely when introducing a concentration of 0.1 mol, it may lead to increased collision rates and higher temperatures up to $T_w = 3400$ K, resulting in a higher Schottky Correction of 4.1 eV. However, with an increase in the electric field, achieved by raising the voltage to $U = 20$ V, as shown in Figure b, there is a noticeable decrease in the ionization

potential to 1.0 V. Additionally, with an increase in concentration, there is an observed rise in the Schottky Correction due to the heightened voltage, which raises the barrier's height, making it more challenging for electrons to move into the metal compared to a voltage of 10 V, consequently leading to a decrease in the ionization potential. These two figures illustrate that for pure xenon, the Schottky value remains relatively low at both voltages of $U = 10$ V and $U = 20$ V. This is accompanied by an increase in ionization potential due to heightened collision processes between molecules and electrons. Consequently, there is a boost in the kinetic energy of the electrons, enhancing their capacity to overcome the Schottky Correction. However, when a concentration of 0.5 mol. is added at both voltages, the opposite effect is observed. The addition of concentration corresponds to an increase in the Schottky Correction (the work function), attributed to collision and liberation processes. At $U = 10$ V, the electrons leading to a rise in current have a Schottky Correction value of 1.8 eV and an ionization potential of 0.3 V. Meanwhile, at $U = 20$ V, the Schottky Correction value stands at 2.8 eV, with an ionization potential of 0.2 V.

CONCLUSIONS

The findings demonstrate that as the temperature of the cathode surface escalates, so does the thermal energy of its material, consequently boosting the kinetic energy of electrons within. This heightened energy prompts electron activation, with more electrons acquiring adequate energy to surpass the work function. Consequently, an increase in emitted electrons occurs alongside elevated average energy and temperature. Conversely, the impact on the voltage barrier is contrary, as heightened energy reduces it, fostering increased ionization processes and electron-molecule collisions. Specifically, applying an electric field at voltages $U = 10$ and 20 V induces a simultaneous rise in atom temperature and Schottky barrier, while lowering the voltage barrier.

Acknowledgments

The authors express their gratitude to Mustansiriyah University (www.uomustansiriyah.edu.iq) in Baghdad, Iraq, for assisting with this study.

REFERENCES

1. Hadi F.M., Ali R.A., Al-Rubaiee A.A. Simulation analyses and investigation of the induced electric field and Ar-Hg mixture on the gas discharge processes. Al-Mustansiriyah J. Sci 2020; 31(3): 126–136.
2. Ali H.J., Ahmed B.M., Khalaf M.K., Albeer A. Plasma Diagnostics of Argon-Oxygen Gases Mixture using Different Applied Power in a DC Sputtering System. Al-Mustansiriyah J. Sci 2023; 34(4): 110–115.
3. Sulaiman S.M., Sulyman S.A.A. The effect of non-thermal plasma Jet on bacterial biofilms and plasmid DNA. Al-Mustansiriyah J. Sci 2021; 32(5): 19–26.
4. Al-Obaidi M.T., Ali R.A., Hamed B. Modelling of Reduced Electric Field and Concentration Influence on Electron Transport Coefficients of He-Ne Plasma. Acta Phys. Pol. A. 2021; 140(4).
5. Temur A.A., Ahmed A.F., Ali R.A. Determination of the Mathematical Model for Plasma Electronic Coefficients of the Earth's Ionosphere. Iraqi J. Sci 2023; 1508–1517.
6. Wharmby D.O. Incandescent, discharge, and arc lamp sources, Handb. Optoelectron. Concepts, Devices, Tech. 2017; 1: 41.
7. Lieberman M.A. Plasma discharges for materials processing and display applications, Adv. Technol. Based Wave Beam Gener. Plasmas 1999; 1–22.
8. Corbella Roca C., Portal S., Kundrapu M., Keidar M. Advances in Synthesis of Nanomaterials By Atmospheric Arc Discharge with Pulsed Power, in Electrochemical Society Meeting Abstracts 242, The Electrochemical Society 2022; 888.
9. Stoffels E. Biomedical applications of electric gas discharges, High Temp. Mater. Process. An Int. Q. High-Technology Plasma Process. 2002; 6(2).
10. Liang P. and Groll R. Numerical study of plasma–electrode interaction during arc discharge in a DC plasma torch. IEEE Trans. Plasma Sci. 2018; 46(2): 363–372.
11. Corbella C., Portal S., Zolotukhin D., Martinez L., Lin L., Kundrapu M., Keidar M. Pulsed anodic arc discharge for the synthesis of carbon nanomaterials, Plasma Sources Sci. Technol. 2019; 28(4): 45016.
12. Li T., Choi S., Watanabe T., Nakayama T., and Tanaka T. Discharge and optical characteristics of long arc plasma of direct current discharge, Thin Solid Films 2012; 523: 72–75.
13. Schwieger J., Baumann B., Wolff M. Arc shape of high-intensity discharge lamps: simulation and experiments," Int. J. Thermophys. 2015; 36: 1327–1335.
14. Benilov M.S. and Cunha M.D. Heating of refractory cathodes by high-pressure arc plasmas: II. J. Phys. D. Appl. Phys. 2003; 36(6): 603.
15. Benilov M.S., Cunha M.D., Naidis G.V. Modelling interaction of multispecies plasmas with thermionic cathodes, Plasma Sources Sci. Technol. 2005; 14(3), 517.

16. Hirschler R., Oliveira D.F., Lopes L.C. Quality of the daylight sources for industrial colour control, Color. Technol. 2011; 127(2): 88–100.
17. Von Keudell A. and Schulz-Von Der Gathen V. Foundations of low-temperature plasma physics – an introduction, Plasma Sources Sci. Technol. 2017; 26(11): 113001.
18. Bellan P.M. Fundamentals of plasma physics. Cambridge university press 2008.
19. Almeida P.G.C., Benilov M.S., Cunha M.D. Formation of stationary and transient spots on thermionic cathodes and its prevention, J. Phys. D. Appl. Phys. 2008; 41(14), 144004.
20. Benilov M.S. and Marotta A. A model of the cathode region of atmospheric pressure arcs, J. Phys. D. Appl. Phys. 1995; 28(9): 1869.
21. Redwitz M., Dabringhausen L., Lichtenberg S., Langenscheidt O., Heberlein J. and Mentel J. Arc attachment at HID anodes: measurements and interpretation, J. Phys. D. Appl. Phys. 2006; 9(10): 2160.
22. Sharma B.L. Metal-semiconductor Schottky barrier junctions and their applications. Springer Science & Business Media 2013.
23. Kim J. Yun J.-H., Kim C.H., Park Y.C., Woo J.Y., Park J., Lee J.-H., Yi J. and Han C.-S. ZnO nanowire-embedded Schottky diode for effective UV detection by the barrier reduction effect, Nanotechnology 2010; 21(11): 115205.
24. Balkanski M. and Wallis R.F. Semiconductor physics and applications, Oxford University Press 2000; 8.
25. Liu Y., Guo J., Zhu E., Liao L., Lee S.-J., Ding M., Shakir I., Gambin V., Huang Y., Duan X. Approaching the Schottky–Mott limit in van der Waals metal–semiconductor junctions, Nature, 2018, 557(7707): 696–700.